

NASA TECHNICAL MEMORANDUM



NASA TM X-1451

NASA TM X-1451

GPO PRICE \$ _____

CFSTI PRICE(S) \$ 3.00

Hard copy (HC) _____

Microfiche (MF) .65

ff 653 July 65

FACILITY FORM 602

N67-35616

(ACCESSION NUMBER)

37
(PAGES)

(THRU)

(CODE)

32

(NASA CR OR TMX OR AD NUMBER)

(CATEGORY)

FLIGHT TEST OF A 30-FOOT-NOMINAL-DIAMETER
DISK-GAP-BAND PARACHUTE DEPLOYED AT
A MACH NUMBER OF 1.56 AND A DYNAMIC
PRESSURE OF 11.4 POUNDS PER SQUARE FOOT

by Clinton V. Eckstrom and John S. Preisser

Langley Research Center

Langley Station, Hampton, Va.

NATIONAL AERONAUTICS AND SPACE ADMINISTRATION • WASHINGTON, D. C. • SEPTEMBER 1967

NASA TM X-1451

**FLIGHT TEST OF A 30-FOOT-NOMINAL-DIAMETER DISK-GAP-BAND
PARACHUTE DEPLOYED AT A MACH NUMBER OF 1.56 AND A
DYNAMIC PRESSURE OF 11.4 POUNDS PER SQUARE FOOT**

By Clinton V. Eckstrom and John S. Preisser

**Langley Research Center
Langley Station, Hampton, Va.**

Technical Film Supplement L-968 available on request.

NATIONAL AERONAUTICS AND SPACE ADMINISTRATION

**For sale by the Clearinghouse for Federal Scientific and Technical Information
Springfield, Virginia 22151 - CFSTI price \$3.00**

FLIGHT TEST OF A 30-FOOT-NOMINAL-DIAMETER DISK-GAP-BAND
PARACHUTE DEPLOYED AT A MACH NUMBER OF 1.56 AND A
DYNAMIC PRESSURE OF 11.4 POUNDS PER SQUARE FOOT

By Clinton V. Eckstrom and John S. Preisser
Langley Research Center

SUMMARY

A 30-foot (9.1 meter) nominal-diameter disk-gap-band parachute (reference area 707 sq ft (65.7 m²)) was flight tested with a 200-pound (90.7 kg) instrumented payload as part of the NASA Planetary Entry Parachute Program. A deployment mortar ejected the test parachute when the payload was at a Mach number of 1.56 and a dynamic pressure of 11.4 lb/sq ft (546 N/m²) at an altitude of 127 500 feet (38.86 km). The parachute reached suspension line stretch in 0.37 second resulting in a snatch force loading of 1270 pounds (5650 N). Canopy inflation began 0.10 second after line stretch. A delay in the opening process occurred and was apparently due to a momentary interference of the glass-fiber shroud used in packing the parachute bag in the mortar. Continuous canopy inflation began 0.73 second after initiation of deployment and 0.21 second later full inflation was attained for a total elapsed time from mortar fire of 0.94 second. The maximum opening load of 3915 pounds (17 400 N) occurred at the time the canopy was first fully opened. The parachute exhibited an average drag coefficient of 0.52 during the deceleration period and pitch-yaw oscillations of the canopy were less than 5°. During the steady-state descent portion of the test period, the average effective drag coefficient was about 0.47 (based on vertical descent velocity and total system weight).

INTRODUCTION

The NASA Planetary Entry Parachute Program (PEPP) was established to provide test data on several parachute configurations for applications in low density environments (ref. 1). The Voyager program, for example, has immediate requirements for such data. The disk-gap-band (DGB) parachute was originally designed for and used as a decelerator for high-altitude meteorological rocket systems (ref. 2) and it was therefore a logical candidate for testing. References 3 and 4 report on earlier PEPP tests of parachutes of ringsail design.

The DGB parachute was designed to meet the goal of aerodynamic stability at all altitudes in combination with good drag efficiency in a configuration that had a minimum

of panels, tapes, seams, and joints (ref. 5). This design was accomplished with the use of two relatively simple parts, the disk and the band, to give both canopy shaping and a geometric opening which is the gap between the disk and the band.

The flight test conditions of interest to the program are deployment at low supersonic Mach numbers and low dynamic pressures which can be achieved at earth altitudes above 100 000 feet (30.5 km). The deployment conditions selected for this flight test were a Mach number of 1.6 and a dynamic pressure of 10 lb/sq ft (479 N/m²). The test was performed by utilizing the rocket launch method described in reference 2. The parachute was deployed unreefed and the test objectives were to observe the dynamics of parachute deployment and inflation and to measure opening shock loads, parachute drag efficiency, and stability characteristics.

A motion-picture film supplement has been prepared and is available on loan. The film shows deployment and inflation of the test parachute and was taken from an onboard camera.

SYMBOLS

| | |
|--------------------------|---|
| $C_{D,o}$ | drag coefficient |
| $(C_{D,o})_{\text{eff}}$ | effective drag coefficient (based on vertical descent velocity) |
| D | drag force, lb (N) |
| D_o | nominal diameter, $\left(\frac{4S_o}{\pi}\right)^{1/2}$, ft (m) |
| g | acceleration due to gravity, 32.2 ft/sec ² (980 cm/sec ²) |
| M | Mach number |
| q_∞ | free-stream dynamic pressure, lb/ft ² (N/m ²) |
| S_o | nominal surface area of parachute canopy (includes gap and vent), ft ² (m ²) |
| S_p | projected area of parachute canopy, ft ² (m ²) |
| t | time from vehicle lift-off, sec |
| t' | time from mortar firing, sec |

| | |
|---------------|---|
| W | weight, lb (kg) |
| \dot{z}_E | vertical descent velocity, ft/sec (m/s) |
| ρ_∞ | free-stream atmospheric density, slugs/ft ³ (kg/m ³) |

TEST SYSTEMS DESCRIPTION

The test payload was carried aloft by an Honest John-Nike rocket system. A photograph of the vehicle configuration is presented in figure 1. The vehicle was unguided but spin stabilization was achieved by canting the Nike fins. The ballast section was tailored to other trajectory parameters so that the payload containing the test parachute would attain the proper velocity at the test altitude. Payload separation from the second-stage Nike rocket was initiated by an onboard timer and effected by means of a pressurized bellows. A radio command system was used to start a programmer which initiated the firing of the parachute deployment mortar. A real-time visual display of the variation of altitude with velocity for the payload, such as is described in references 2 and 3, was used in conjunction with Mach number and dynamic-pressure grids to determine the proper time for transmitting the radio command signal.

A diagram of the test payload is presented in figure 2. The payload contained two backup or recovery parachutes which could be deployed by radio command at any time after payload separation if the performance of the test parachute was such that the anticipated impact velocity would be great enough to cause damage to the payload. The weight of the test payload was approximately 200 pounds (90.7 kg); total descent weight including the test parachute was 226 pounds (103 kg).

Onboard instrumentation consisted of a tensiometer placed in the parachute riser line, a $\pm 75g$ range accelerometer aligned with the longitudinal axis of the vehicle, two $\pm 5g$ range accelerometers mounted perpendicular to the longitudinal axis, an attitude reference system, and two cameras. The attitude reference system, commonly referred to as a gyro platform, was included to record payload motions in pitch, yaw, and roll during the test. However, the gyro platform malfunctioned immediately after second-stage ignition; thus, no gyro data were available for parachute stability analysis. It was therefore necessary to depend on camera film data alone for stability analysis. The resolution of data is not as good when camera film is used and some uncertainty is introduced by not having a well-defined inertial reference such as the gyro platform would provide. One of the two cameras was mounted in a pod on the payload (see fig. 2) and pointed aft to record parachute performance. The second camera was mounted in the nose of the payload and pointed forward so that it would provide data on payload motions relative to earth during the descent portion of the test.

The tensiometer, accelerometer, and gyro-platform measurements were telemetered to ground receiving stations and recorded on magnetic tape. Camera film was obtained from the recovered payload.

TEST PARACHUTE DESCRIPTION

The test parachute was a disk-gap-band (DGB) design having a nominal diameter D_0 of 30 feet (9.1 m) and a reference area of 707 square feet (65.7 m²). Figure 3 shows the dimensional details of a gore and the general parachute-payload configuration. The in-flight diameter of the disk-gap-band parachute was about 20 feet (6.1 m). The parachute had 24 gores and a geometric porosity or open area of 15 percent. The gap alone provided 14.5 percent geometric porosity; the remaining porosity was located in the crown of the canopy in the form of a vent. The parachute was equipped with a torus inflation aid; however, the torus pressurization system was not activated during this flight test.

The parachute, with the exception of the torus, was fabricated entirely of dacron materials. Suspension lines were coreless braided dacron having a rated tensile strength of 550 pounds (2447 N). The canopy disk and band gore panels were fabricated of two sections each with the material warp and fill threads running 45° to the center line of the gore.

The canopy vent edge was reinforced with three layers of 3/4-inch (1.91 cm) wide dacron tape of 550-pound (2447 N) rated tensile strength. The outer edge of the disk portion of the canopy and both edges of the band were reinforced with a single 3/4-inch (1.91 cm) wide 550-pound (2447 N) rated tensile strength dacron tape. The gore edges were joined by a french fell seam (ref. 6) and reinforced with a 3/4-inch (1.91 cm) wide radial tape of 550-pound (2447 N) rated tensile strength dacron. Each radial tape was continuous up the full length of the gore, across the vent and down the gore seam on the opposite side of the canopy. At the lower edge of the band the radial tape formed a loop and was sewn back 4 inches (10.2 cm) on the inside surface of the band. This loop was used for attachment of the suspension lines. The radial tape was a double thickness across the gap between the band and the disk.

The parachute attachment system, shown in figure 3, consisted of an upper riser, an explosive-bolt-actuated disconnect link, an intermediate riser, a tensiometer, and a bridle. The upper riser was 4 feet (1.2 m) in length and attached to the suspension lines by four metal connector links with 6 lines on each link. The tensiometer and the disconnect link were each approximately 1/2 foot (0.15 m) long. The intermediate riser was 2 feet (0.61 m) in length. The bridle consisted of a single line for $1\frac{1}{2}$ feet (0.46 m);

this line then separated into three legs, each of which was 3 feet (0.91 m) long. The bridle provided a three-point attachment to the payload. The upper riser, the intermediate riser, and the single line portion of the bridle consisted of four layers of $1\frac{3}{4}$ -inch (4.45 cm) wide low-elongation dacron webbing of 7000-pound (31 140 N) rated tensile strength. Each of the three legs of the bridle was a single thickness of 7000-pound (31 140 N) rated webbing.

The weight of the parachute including the attachment hardware was 26 pounds and it was packed to a density of 40 pounds per cubic foot (641 kg/m^3) in a cylindrical dacron bag which was closed with a bag mouth tie. No canopy or suspension line holders or restraints were used inside the deployment bag except for a 300-pound (1335 N) rated break line from the apex of the canopy to the bottom of the bag. The entire deployment bag including the mouth closure was lined with cotton cloth to prevent friction burning during packing and deployment. A glass-fiber shroud was placed over the mouth end of the bag to protect it during mortar fire. The mortar deployment method used was described in detail in reference 3.

The parachute was equipped with a system of lines which allowed it to be reefed after the data period was completed. This system of lines was termed a "post-reefing" system since the parachute was not reefed during the actual test. Post-reefing serves to increase the parachute descent rate, and thereby reduces the total flight time and the corresponding drift due to winds.

The packed parachute and deployment bag were subjected to a temperature of 125°C for 120 hours. This heat cycle is representative of part of the sterilization requirements for equipment to be used in interplanetary spacecraft and therefore was included as part of the test requirements so that any resulting degradation of the physical properties of the parachute could be evaluated.

PREFLIGHT TESTS

A series of three deployment tests of the DGB flight configuration were conducted from the whirlltower test facility at El Centro, California, during July of 1966 in preparation for the rocket flight test. The purpose of these tests was to evaluate the parachute structural design and to determine opening characteristics of the DGB parachute. A photograph taken during these tests showing the test parachute in a near fully inflated condition is presented in figure 4. The tests were performed by locating the test parachute and the payload in the gondola which hangs from the whirlltower arm by a cable. When the desired airspeed was attained, the payload was released from the gondola. The packed parachute was then ejected from the payload by a mortar system similar to that used in the flight tests.

The whirltower tests were conducted at near sea-level conditions with various release velocities. The following table lists the snatch forces and opening shocks measured during these tests:

| Test | Release velocity | | Dynamic pressure | | Snatch force | | Opening shock | |
|------|------------------|-------|------------------|------------------|--------------|------|---------------|------|
| | ft/sec | m/sec | lb/sq ft | N/m ² | lb | N | lb | N |
| 1 | 170 | 51.8 | 33 | 1580 | 1200 | 5338 | 1125 | 5004 |
| 2 | 230 | 70.1 | 57 | 2729 | 1150 | 5115 | 1500 | 6672 |
| 3 | 320 | 97.5 | 112 | 5363 | No data | | | |

The canopy and suspension lines suffered no structural damage during the three deployment tests. A torus inflation aid was located on the inside surface of the band, since the original intention was to use such a device in the parachute for the flight test. On two of the three deployment tests, the torus suffered some damage. (See fig. 4.) The inflation aid was subsequently redesigned and subjected to additional tests in the 60-foot (18.3 m) vacuum sphere at NASA Langley Research Center prior to fabrication of the flight parachute. Although a torus was included in the flight article, it was not inflated during the flight test since just prior to the flight it was decided to study canopy inflation for this test without the aid of any mechanical device.

RESULTS AND DISCUSSION

Test Data

The flight test vehicle was launched at 10:12 a.m. m.s.t. on December 10, 1966, at White Sands Missile Range, New Mexico. The recorded times for the important flight events are listed on the right-hand side of figure 5. Time histories of the altitude and relative velocity from vehicle lift-off through the parachute test period are shown in figure 6. The test period begins at parachute deployment and terminates with the post-reefing function.

An Arcas meteorological sounding rocket was launched 1 hour after the flight test to measure upper-altitude winds and temperatures. This information was supplemented by a radiosonde 1 hour and 27 minutes before the flight test. Upper atmospheric winds as determined from the rocket sounding are presented in figure 7. Temperature information from both soundings is presented in figure 8, and atmospheric density as derived from the measured temperatures is presented in figure 9. Data from the sounding rocket were used for calculations down to an altitude of 85 000 feet (25 900 m). Below 85 000 feet the radiosonde data were used.

The measured atmospheric data were used with radar track and telemetered data to determine the payload true airspeed, Mach number, and dynamic pressure (figs. 10 and 11) during the deployment period. The initiation of the deployment sequence or time of deployment is defined by mortar firing (labeled $t' = 0$ on the figures herein). The parachute-payload system altitude during the deployment sequence, as determined by radar tracking, is presented in figure 12. Note that the payload was in the ascent portion of the flight trajectory at the time the parachute was deployed. As indicated in figures 10 to 12, the parachute deployment was initiated at a true airspeed of 1615 ft/sec (491 m/s) ($M = 1.56$) and a dynamic pressure of 11.4 lb/sq ft (546 N/m²) at an altitude of 127 500 feet (38.86 km) above mean sea level.

The true airspeed and Mach number data presented in figure 10 are based on radar tracking up to the instant the deployment mortar was fired. From the time of mortar firing to $t' = 6$ seconds, true airspeed was determined from integrated tensiometer data which was essentially the same as that determined from integrated accelerometer data. Radar tracking data processed to obtain velocity were generally in good agreement with data established by the onboard instrumentation.

The payload velocity increased slightly immediately after initiation of the deployment sequence because of the reaction on the payload due to the firing of the mortar. The velocity decay associated with inflation of the parachute began at about $t' = 0.77$ second, the greatest decrease in velocity occurring at about $t' = 0.94$ second. After this time, the parachute was fully opened and the system velocity decreased rapidly to 800 ft/sec (244 m/s) at $t' = 3.0$ seconds. Apogee occurred at approximately 134 800 feet (41.09 km) as shown in figure 12, and the true airspeed at this time was 242 ft/sec (73.8 m/s).

The time history of force transmitted through the riser line as measured by the tensiometer during the deployment period is presented in figure 13. The double peak forces of 480 pounds (2135 N) and 560 pounds (2490 N) at $t' = 0.17$ and 0.21 second are attributed to the full length deployment of the parachute attachment bridle and then the risers. The peak force of 1270 pounds (5650 N) which occurred at $t' = 0.37$ second was the snatch force associated with stretching of the suspension lines. The force buildup associated with parachute opening started at $t' = 0.77$ second and reached a maximum of 3915 pounds (17 400 N) at $t' = 0.94$ second. The force decreased rapidly to 1400 pounds (6230 N) at $t' = 1.01$ seconds and increased again to 2640 pounds (11 740 N) at $t' = 1.04$ seconds after which the force decreased at a rate corresponding to the decreasing system velocity. The rapid change in force immediately after opening was coincident with parachute shape variations attributed to the dynamics of the opening process.

Figure 14 presents the data obtained from the three orthogonally mounted accelerometers in the payload. Positive longitudinal accelerations imposed by the firing of

the mortar are not shown but were an average of 20g for 0.03 second. The maximum shock of 20.5g occurred at $t' = 0.94$ second and corresponded to full opening of the parachute. The normal acceleration loads indicate payload angular motion which was confirmed by the aft-camera film.

As mentioned previously, gyro platform data were unavailable for analysis of parachute stability. However, during the period immediately following parachute deployment, as the payload-parachute system was still ascending, ground references were visible on the aft-camera film. By utilization of this film, parachute motions relative to earth were measured during the deceleration phase of the test period. For the remainder of the test period, only payload-parachute relative motions were obtained since no earth-fixed references were visible. The aft camera was set at a frame rate of 64 frames per second and approximately 50 seconds of film data were obtained. The nose camera, having a frame rate of 16 frames per second, provided data for approximately 220 seconds. However, payload motions could not be determined until the payload-parachute system had passed apogee and the earth references were clearly visible on the nose-camera film. The nose-camera film which provided data on payload motions relative to the earth was used in comparison with the available aft-camera-film data (which provided relative payload-parachute motions) to determine the stability of the parachute canopy during a portion of the descent phase of the test period.

Parachute Performance

Inflation characteristics.- As mentioned previously, the time from mortar fire to suspension line stretch was 0.37 second; thus, an average ejection velocity of 112 ft/sec (34.1 m/s) was achieved (based on a suspension line length of 30 feet (9.1 m) and an attachment system length of 11.5 feet (3.51 m)). The resulting snatch force load was 1270 pounds (5650 N).

The parachute projected area S_p variation with time was determined from onboard film, several frames of which are shown in figure 15. Drag area development began at $t' = 0.47$ second and continued to $t' = 0.60$ second as shown in figure 16. At this time the drag area decreased. A review of the aft-camera film revealed that the glass-fiber cloth shroud (about $3\frac{1}{2}$ feet square ($\approx 1 \text{ m}^2$)) which was used to protect the deployment bag from the mortar blast, was in close proximity to the parachute suspension lines near the canopy skirt and did not move away from the parachute until after the canopy began the first inflation process. (See fig. 15(a).) Therefore, the interruption in the inflation process evident in figure 16 between $t' = 0.60$ second and $t' = 0.73$ second is attributed to the interference of the glass-fiber shroud. (To prevent recurrence of this problem, the deployment bag has been modified and the glass-fiber shroud has been eliminated for later flight tests.) At $t' = 0.73$ second, the inflation process began again and continued in a normal manner, the first full inflation occurring

at $t' = 0.94$ second. At this time the Mach number was 1.44 and the maximum opening shock load of 3915 pounds ($\approx 17\,400$ N) was recorded. After 0.94 second, oscillatory variations in canopy shape (see fig. 15(b)) occurred for about 0.25 second as shown by the projected area plot in figure 16.

The canopy shape variations were primarily partial inversions of the skirt or band portion of the canopy somewhat similar to the variations noted in reference 3 for the test of a modified ring-sail configuration. Canopy shape variations occurring immediately after a parachute is first fully inflated are normal, however, and are primarily attributed to the rapidly changing airflow pattern around the canopy at this time. It should be noted from figure 16 that the shape variation lasted for less than 0.25 second and that steady full inflation was achieved with only minor variations occurring after $t' = 1.2$ seconds (corresponding to a Mach number of 1.35.)

Drag efficiency.- As described previously, the payload was at a Mach number of 1.56 when parachute deployment was initiated and at a Mach number of 1.44 when the parachute was first fully opened. The system decelerated to subsonic velocities within 1.2 seconds after the parachute was first fully opened (2.15 seconds after mortar deployment). The computed drag coefficient $C_{D,o}$ is presented in figure 17 as a function of Mach number during the deceleration period immediately after deployment. The parachute, which had a total reference area of 707 square feet (65.7 m^2) (including the gap and vent), provided a mean $C_{D,o}$ of about 0.52 during the deceleration period immediately after deployment. (This mean value is an average of all calculated data points.) Drag forces were calculated from both the recorded tensiometer force data and the longitudinal accelerometer data. Since the parachute was decelerating the total system rather than just the payload, the total drag force was larger than the recorded tensiometer force by the ratio of the total system weight to the payload weight (1.12:1.0). The equation used to determine the drag coefficient is as follows:

$$C_{D,o} = \frac{D}{q_{\infty} S_o}$$

Figure 18 presents the vertical descent velocity and "effective" drag coefficient variations with altitude. The effective drag coefficient values are based on steady-state or equilibrium vertical descent velocities and the system weight as shown by the following equation:

$$(C_{D,o})_{\text{eff}} = \frac{2W}{\rho_{\infty} \dot{z}_E^2 S_o}$$

The start of steady-state descent was taken to be the time at which the deceleration of the system became less than $0.1g$. Based on radar tracking data, this time corresponded to an altitude of 125 000 feet (38.1 km).

During steady-state descent, the average effective drag coefficient was about 0.47. A 50 ft/sec (15.2 m/s) increase in velocity and a corresponding decrease in effective drag coefficient occurred at an altitude of approximately 76 000 feet (23.16 km) (fig. 18); this change resulted from the parachute post-reefing function.

Stability.- At the time of mortar fire, the payload roll rate was 5 cycles per second (31 radians per second). Analysis of the aft-camera film revealed that the parachute canopy retained very little of this rolling motion by the time full inflation occurred. The average roll rate of the parachute canopy during a 10-second period after mortar fire was less than 0.2 radian per second and in the same direction as the payload roll. Measured canopy pitch-yaw oscillation angles were between 0° and 5° during this time period.

At $t' = 45$ seconds, the horizontal component of the system velocity had diminished to less than 30 feet per second (9.1 m/sec) and vertical deceleration had become less than $0.1g$. This point was defined as the start of terminal descent. Since the aft-camera coverage was for approximately 50 seconds, limited film data were available for analysis during the terminal descent phase of the trajectory. The aft-camera film provided a measurement of the relative pitch-yaw angle and the relative roll motion between the payload and the parachute canopy. The nose-camera film provided similar attitude data for the payload relative to earth. Figure 19 presents a comparison of pitch-yaw oscillation angles between data obtained from the nose camera and that obtained from the aft camera for the time period from $t' = 45$ seconds to $t' = 50$ seconds. Since the data agree in magnitude within 5° , it can be concluded that the major motion was due to the payload oscillation about the center line of the parachute. The average payload roll rate during this time interval was 1.2 cycles per second. It is known that at least some pitch-yaw payload oscillations were a result of the payload roll which caused the bridle and riser system to wind up. It was also determined from nose-camera-film data that in addition to a pitch-yaw oscillation about the parachute center line, the payload traversed a 5° arc in the vertical plane during this 5-second time interval. This latter motion may be attributed to the parachute and payload moving together in a simple pendulum-type motion.

It was observed from the entire nose-camera-film data that on nine occasions, the payload roll rate diminished to zero; this condition corresponded to those times when the system had absorbed all the payload roll energy and was fully wound up and when the system was fully wound up in the opposite direction after unwinding. However, no consistent pattern of payload motions could be ascertained at these times and therefore a detailed payload-parachute system motion description could not be formulated.

Parachute damage analysis.- The test parachute shown in figure 20 suffered no visible damage during deployment. However, one suspension line and one suspension-

line attachment loop were severed prior to recovery and are assumed to have been damaged during the post-reefing operation which occurred after the test period was completed. This damage was caused by friction burning and did not adversely affect the operation of the post-reefing system and the desired increase in descent velocity was achieved with a resultant on range impact and recovery.

CONCLUSIONS

The 30-foot (9.1 meter) nominal diameter disk-gap-band parachute was flight tested with a 200-pound (90.7 kg) rocket-launched instrumented payload. The deployment occurred at an altitude of 127 500 feet (38.86 km) at a Mach number of 1.56 and a dynamic pressure of 11.4 lb/sq ft (546 N/m²). Based on an analysis of the data acquired, the following conclusions are made:

1. The mortar deployment system operated correctly and the time from deployment to suspension line stretch was 0.37 second.
2. The deployment snatch force load associated with suspension line stretch was 1270 pounds (5650 N).
3. The test parachute was fully inflated in less than 1 second and the opening load was 3915 pounds (17 400 N).
4. The parachute exhibited an average drag coefficient of 0.52 during the deceleration period and an average effective drag coefficient of 0.47 during steady-state descent.
5. From analysis of the payload camera films, it is concluded that the parachute motions were less than $\pm 5^\circ$ during the deceleration period and during that portion of the descent where data were available.

Langley Research Center,
National Aeronautics and Space Administration,
Langley Station, Hampton, Va., August 10, 1967,
709-08-00-01-23.

REFERENCES

1. McFall, John C., Jr.; and Murrow, Harold N.: Parachute Testing at Altitudes Between 30 and 90 Kilometers. AIAA Aerodynamic Deceleration Systems Conference, Sept. 1966, pp. 116-121.
2. Eckstrom, Clinton V.: Development and Testing of the Disk-Gap-Band Parachute Used for Low Dynamic Pressure Applications at Ejection Altitudes at or Above 200,000 Feet. NASA CR-502, 1966.
3. Preisser, John S.; Eckstrom, Clinton V.; and Murrow, Harold N.: Flight Test of a 31.2-Foot-Diameter Modified Ringsail Parachute Deployed at a Mach Number of 1.39 and a Dynamic Pressure of 11 Pounds Per Square Foot. NASA TM X-1414, 1967.
4. Whitlock, Charles H.; Bendura, Richard J.; and Coltrane, Lucille C.: Performance of a 26-Meter-Diameter Ringsail Parachute in a Simulated Martian Environment. NASA TM X-1356, 1967.
5. Murrow, Harold N.; and Eckstrom, Clinton V.: Description of a New Parachute Designed for Use With Meteorological Rockets and a Consideration of Improvements in Meteorological Measurements. AMS/AIAA Paper No. 66-399, Mar. 1966.
6. Anon.: Performance of and Design Criteria for Deployable Aerodynamic Decelerators. ASD-TR-61-579, U.S. Air Force, Dec. 1963.



Figure 1.- Photograph of vehicle configuration. U.S. Army photograph.

L-67-6624

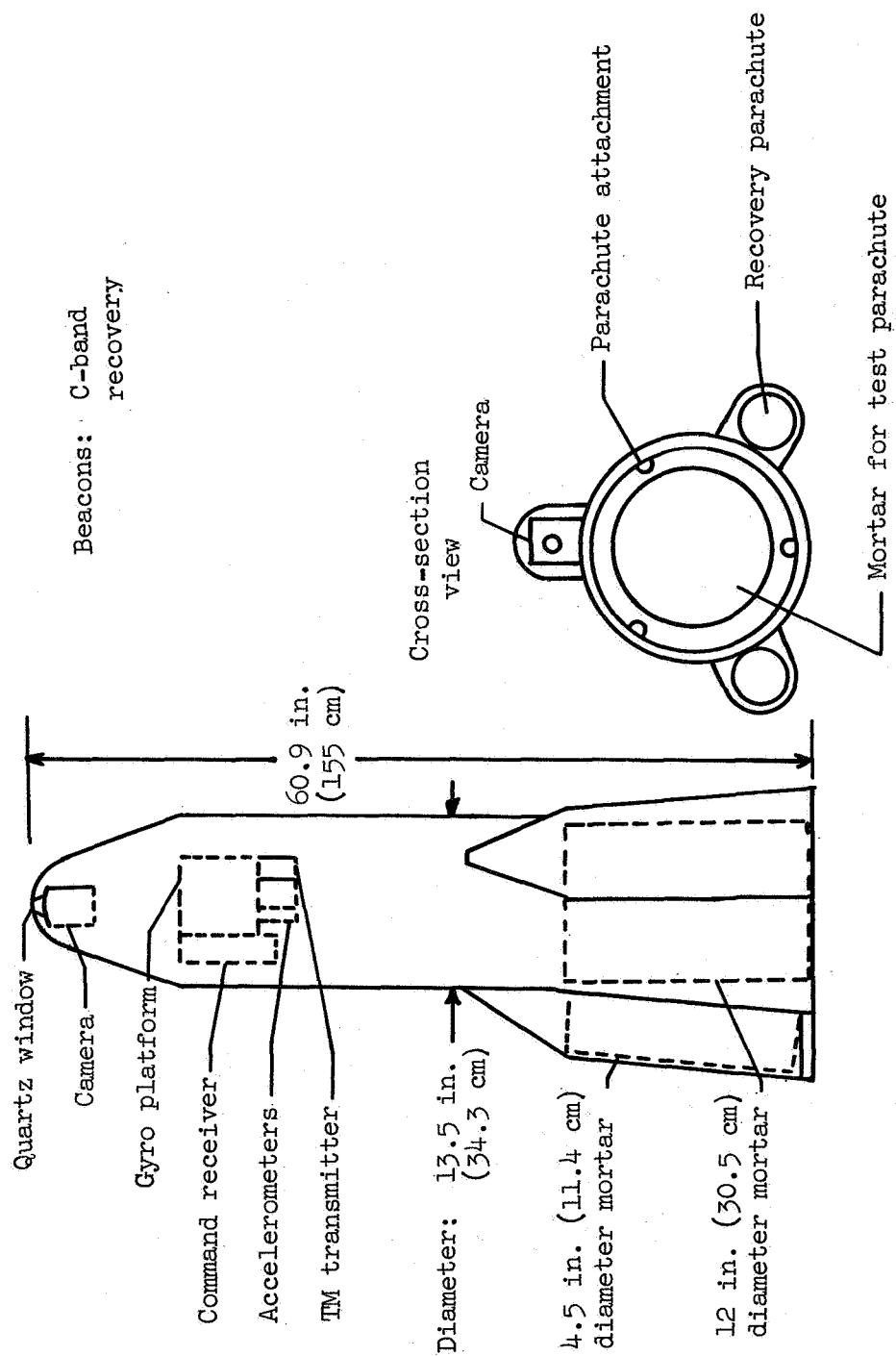
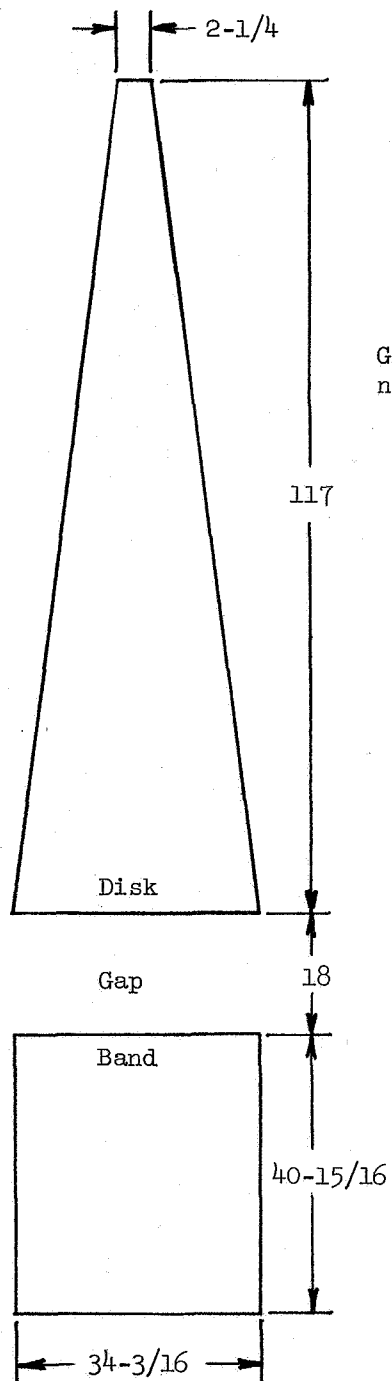
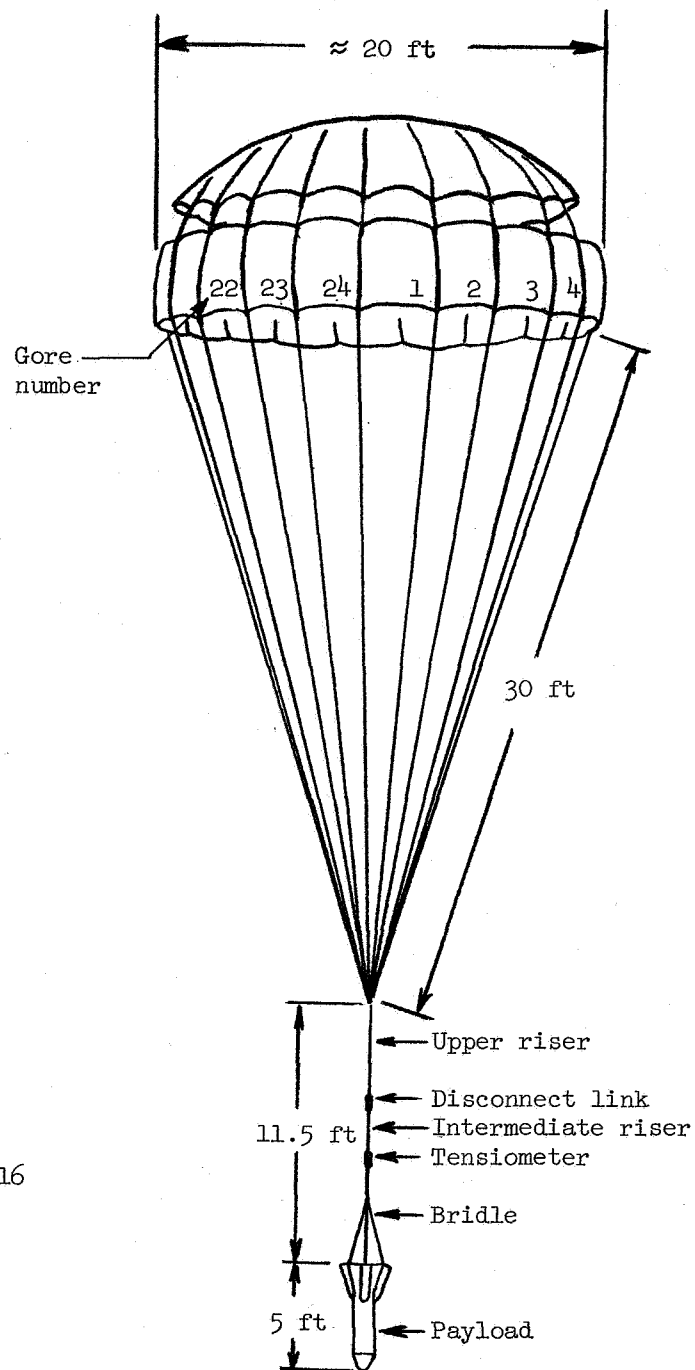


Figure 2.- Test payload.



Gore dimensional details



Flight configuration

Figure 3.- Disk-gap-band parachute gore dimensional details and flight configuration.

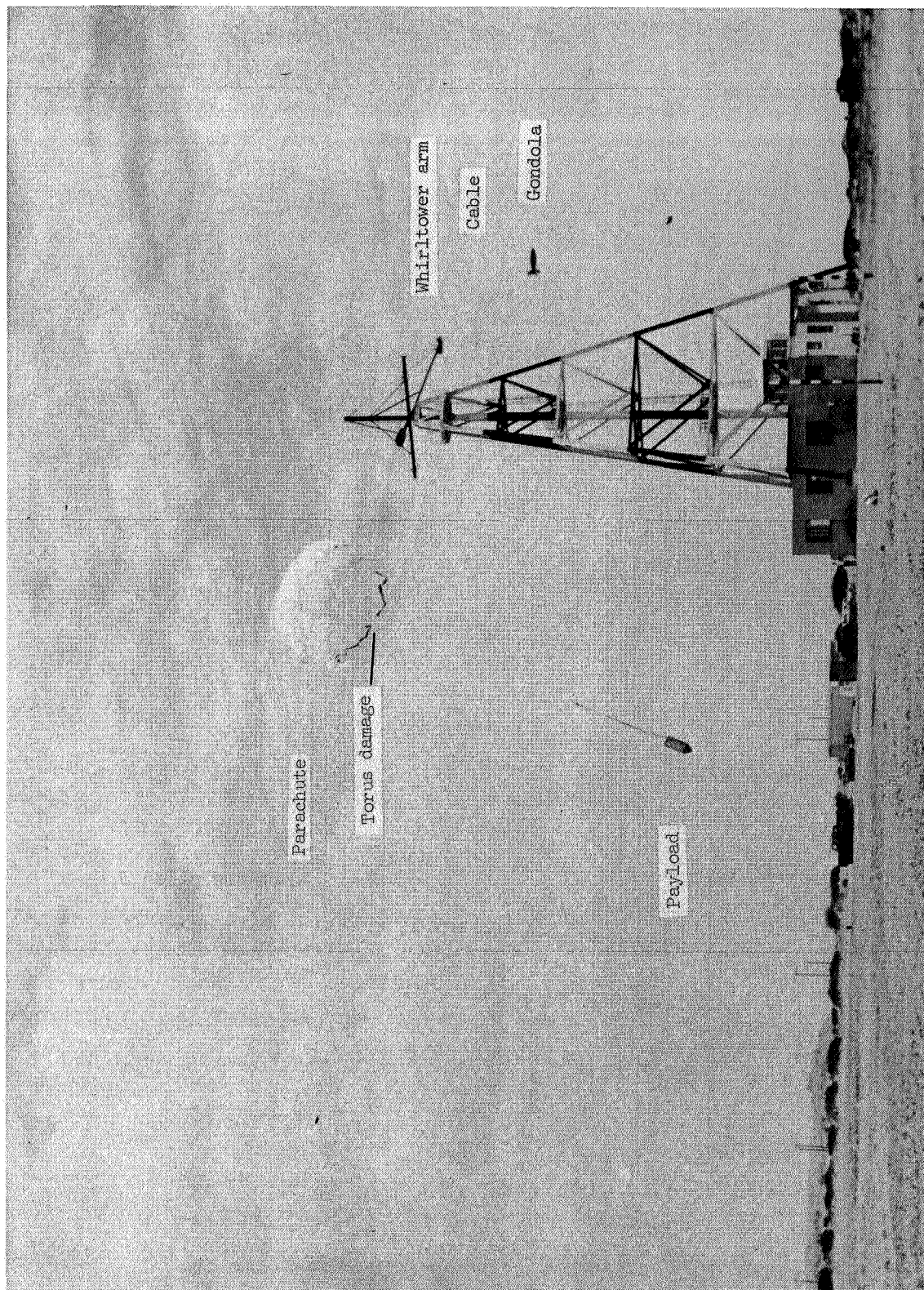


Figure 4.- Photograph of preflight test at the whirtower test facility.

L-66-8257.1

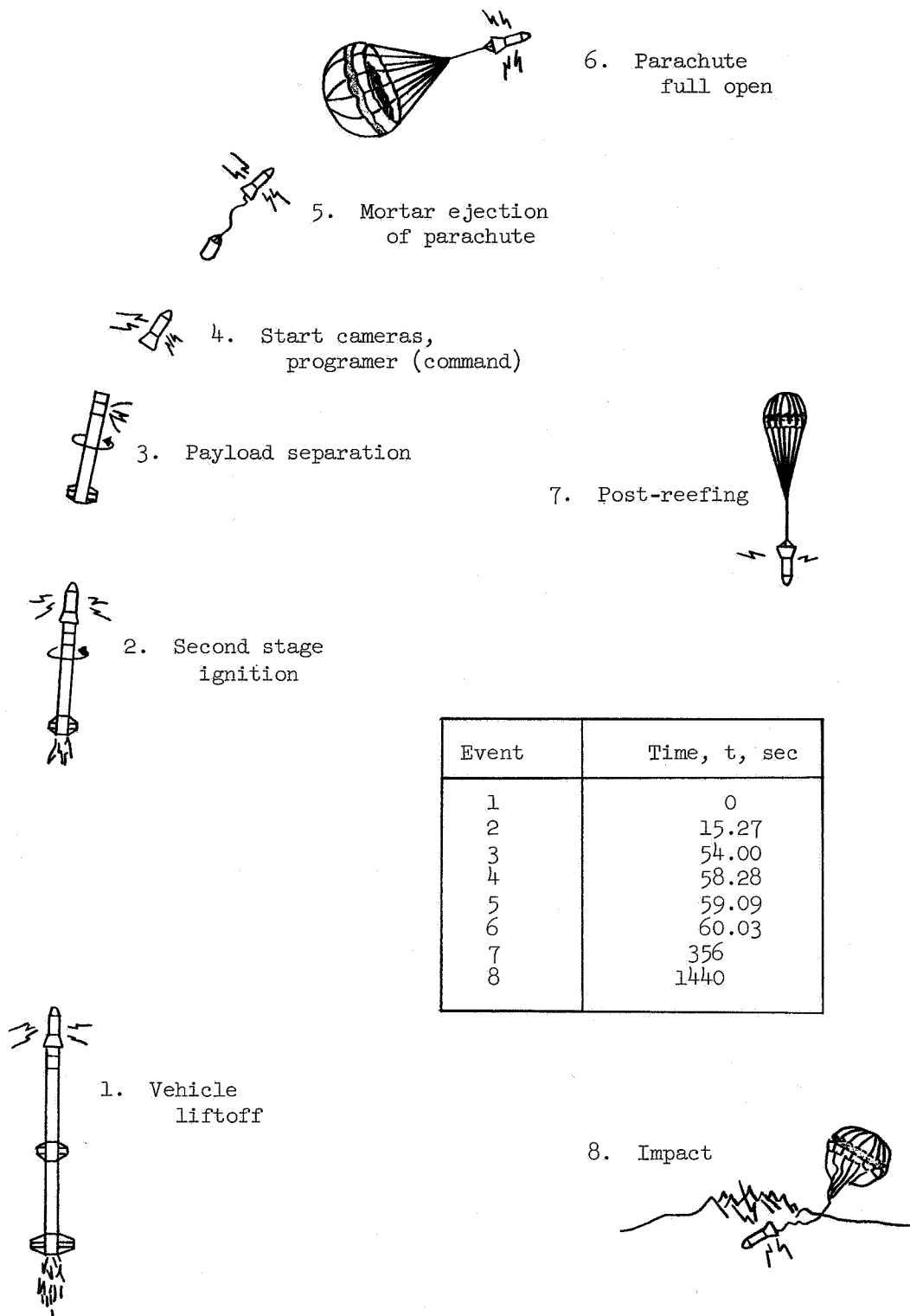


Figure 5.- Flight sequence of events.

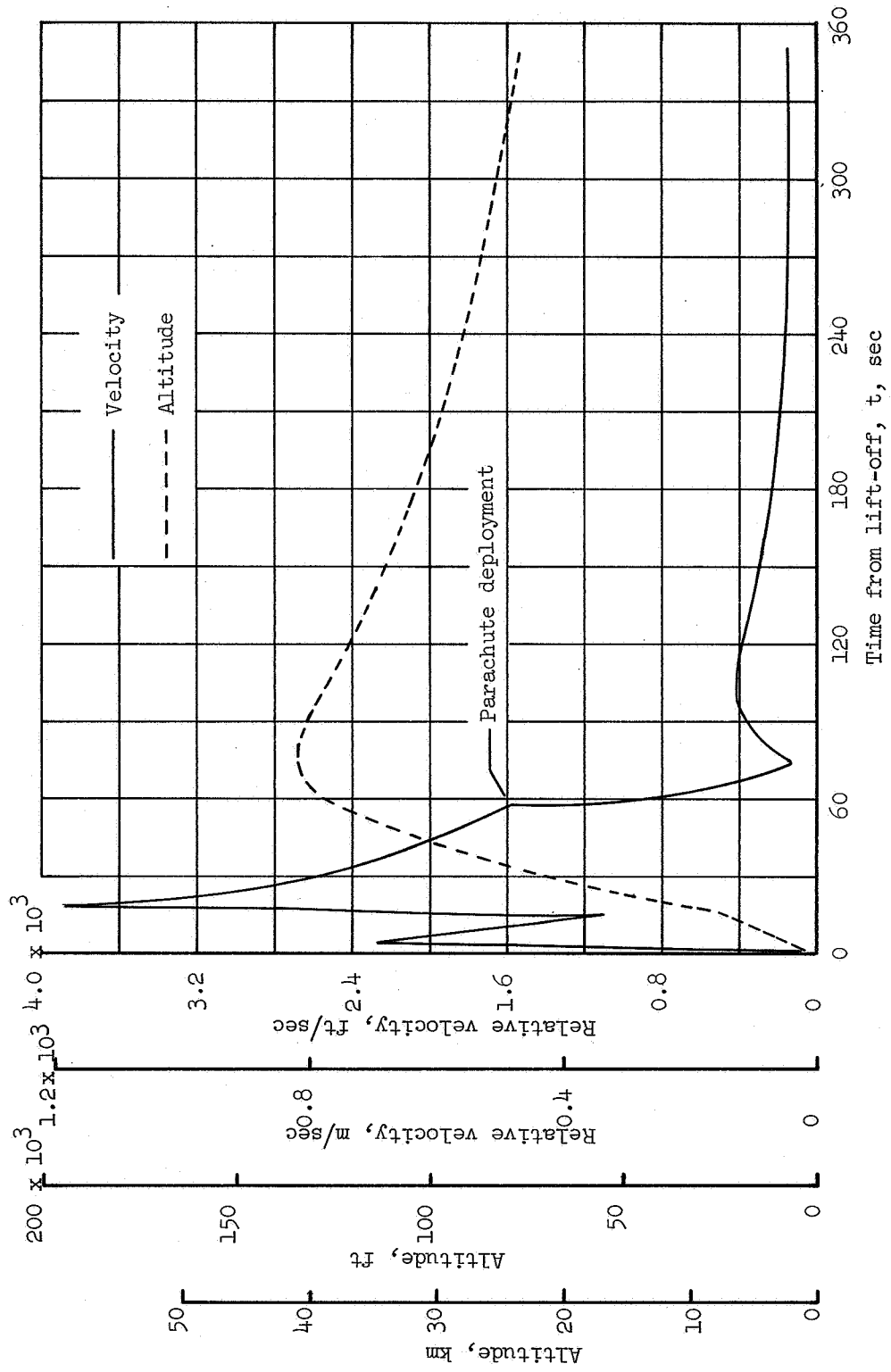


Figure 6.- Time histories of altitude and relative velocity.

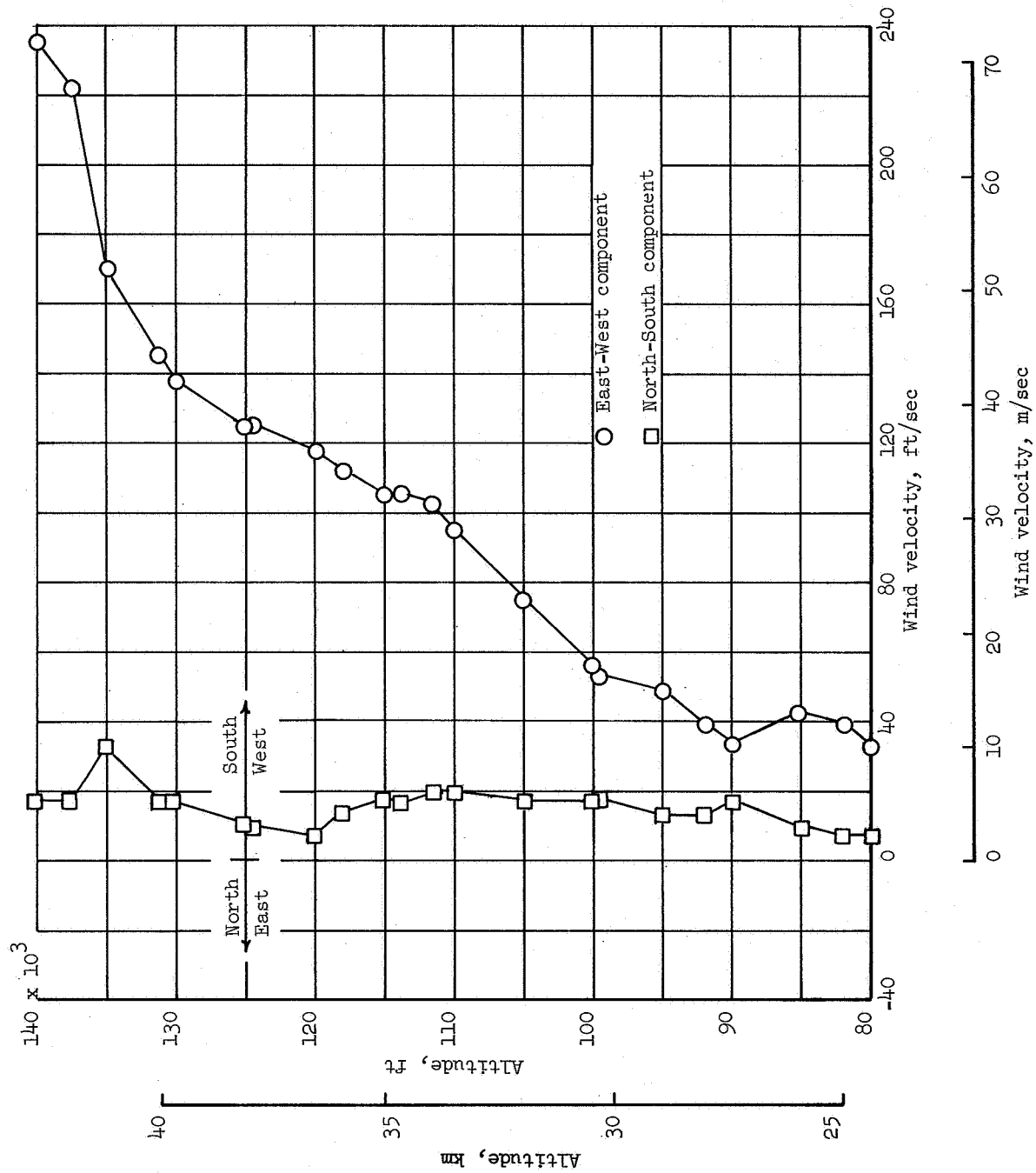


Figure 7.- Wind-velocity profile in north-south and east-west components.

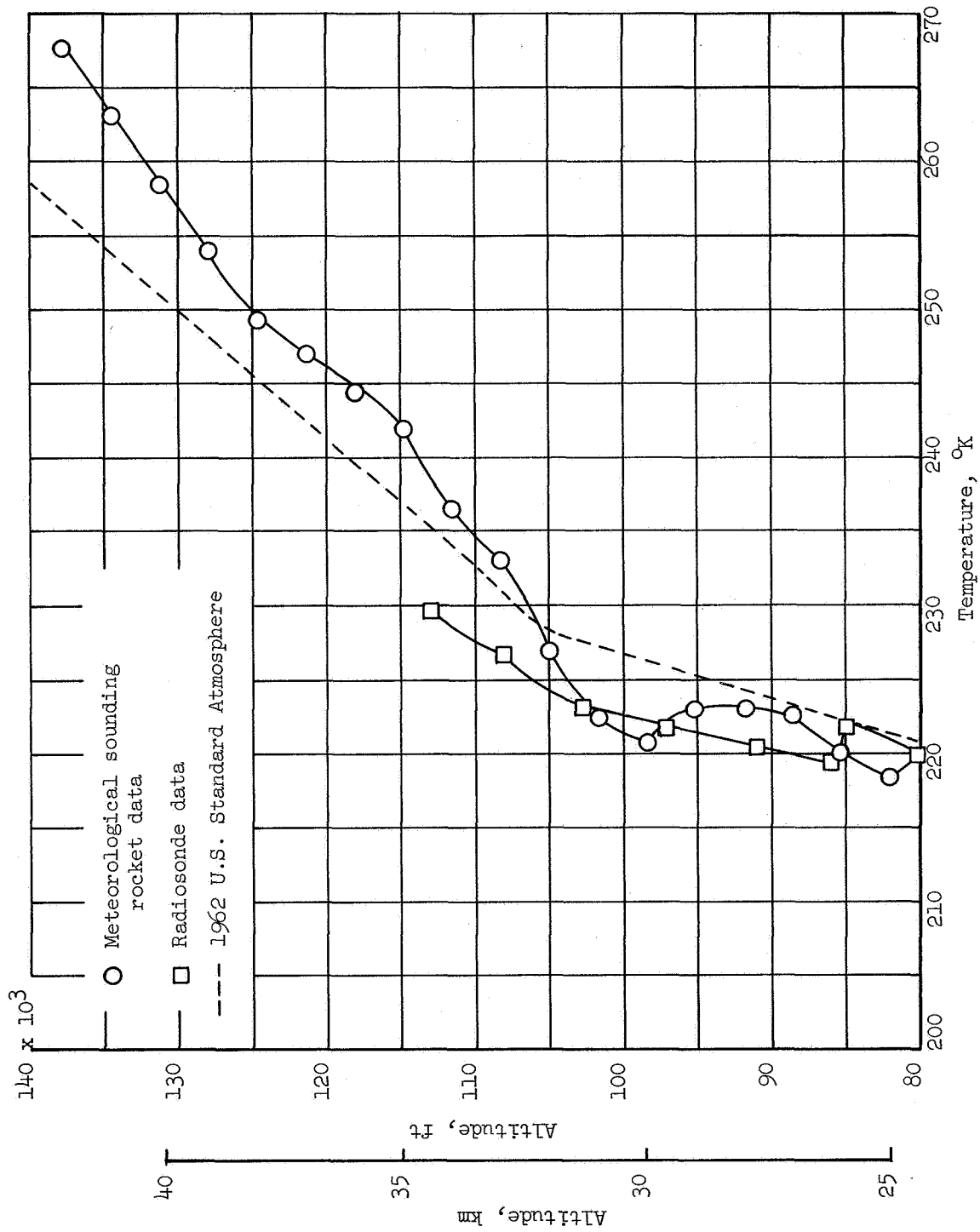


Figure 8.- Atmospheric temperature profile.

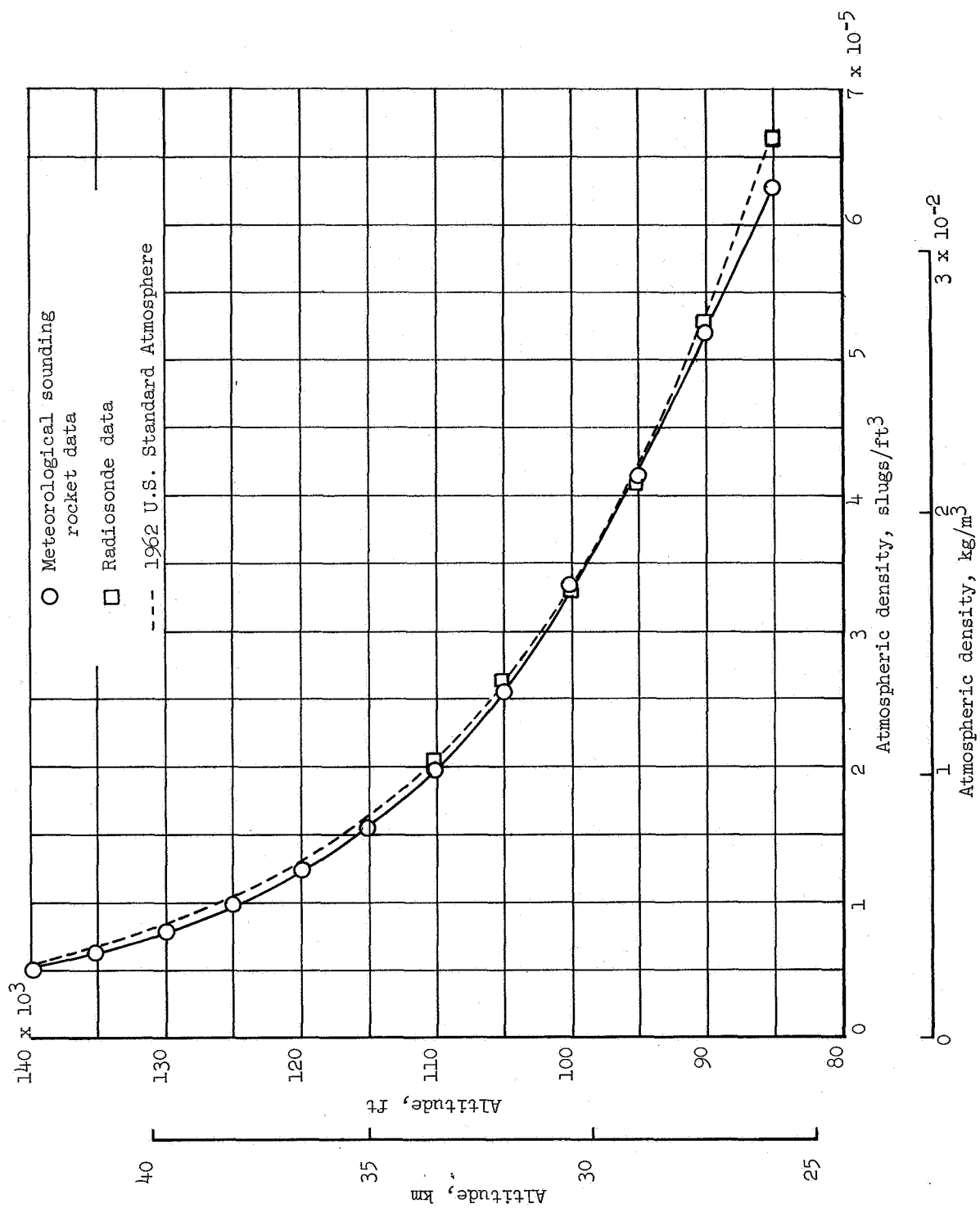


Figure 9.- Atmospheric density profile.

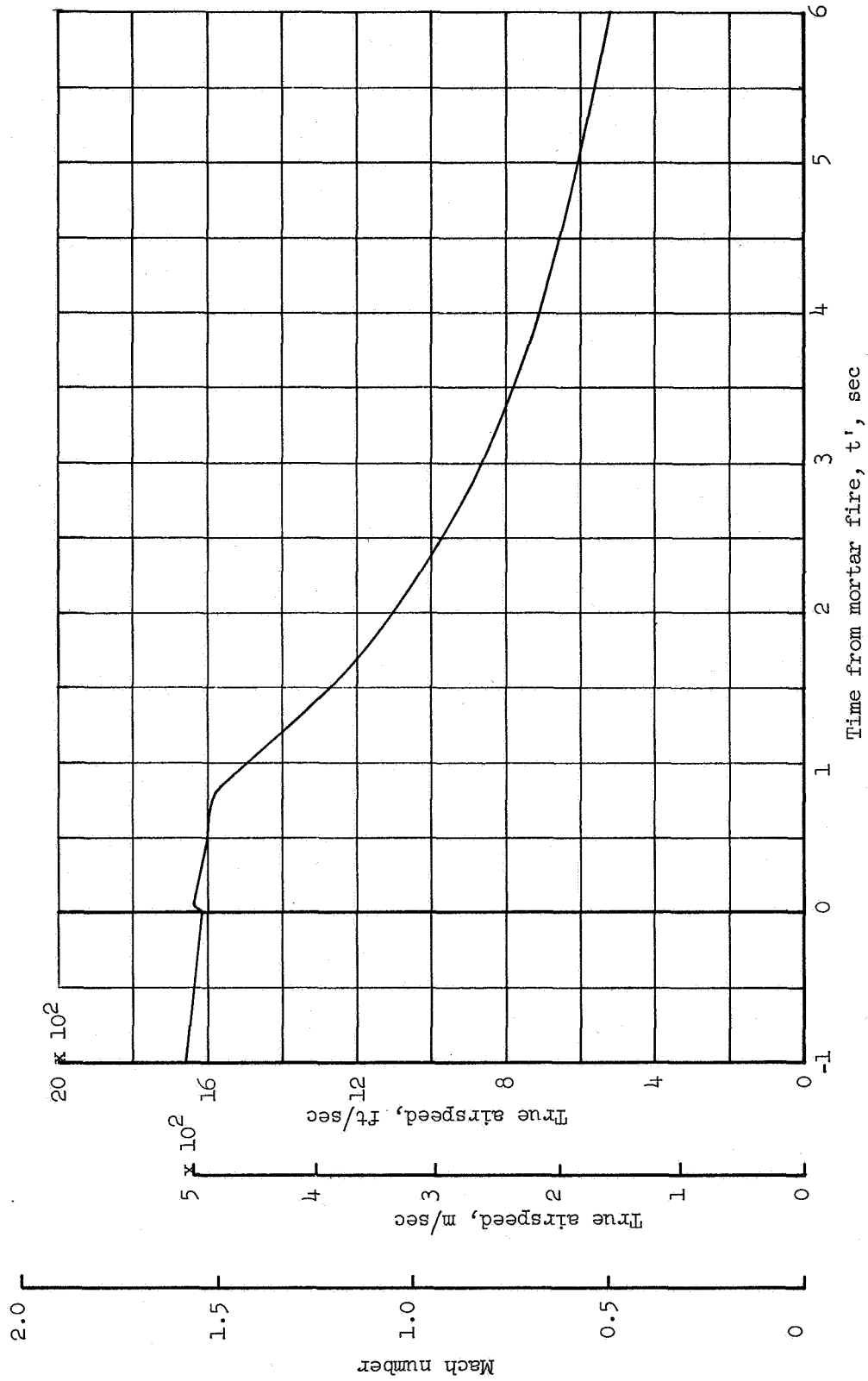


Figure 10.- Mach number and true airspeed time histories.

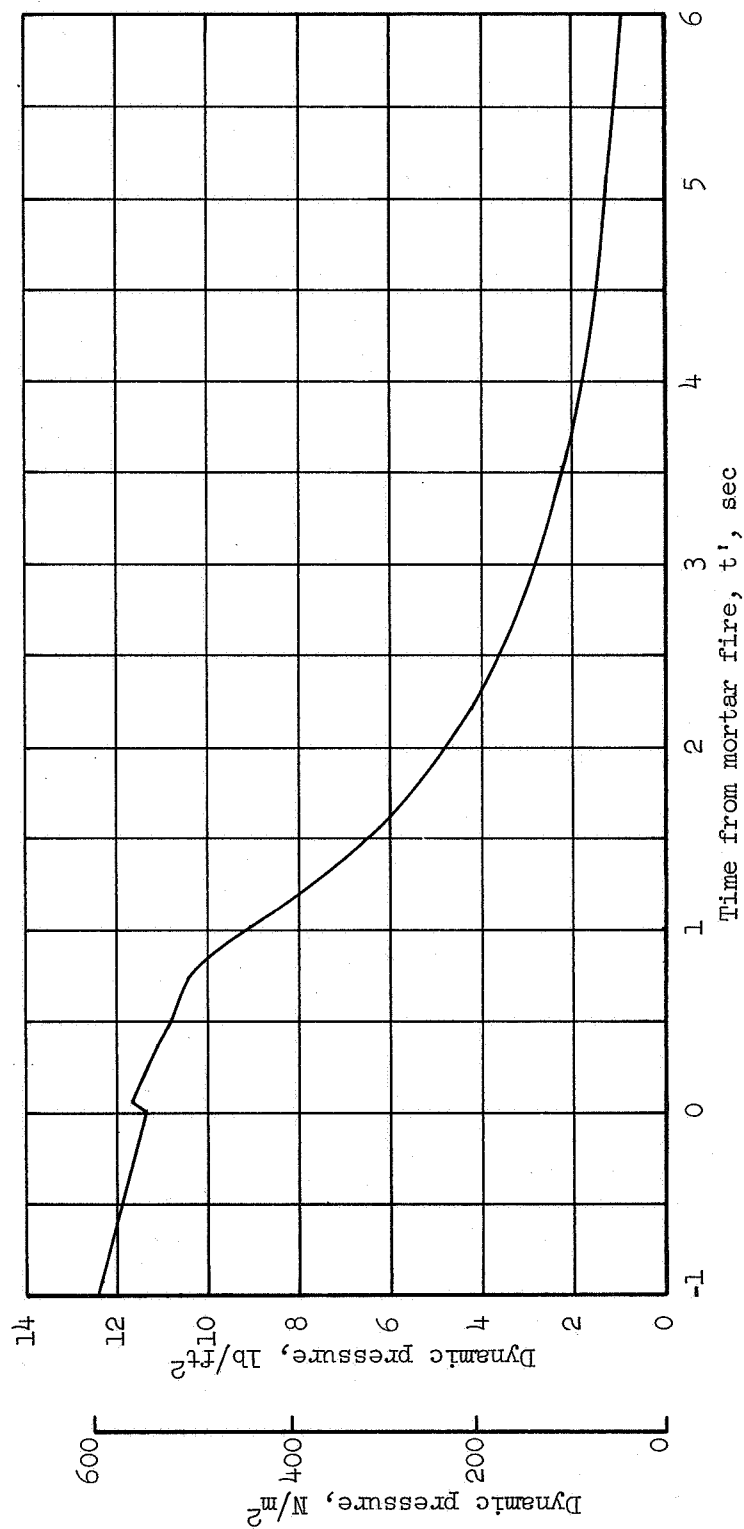


Figure 11.- Dynamic pressure time history.

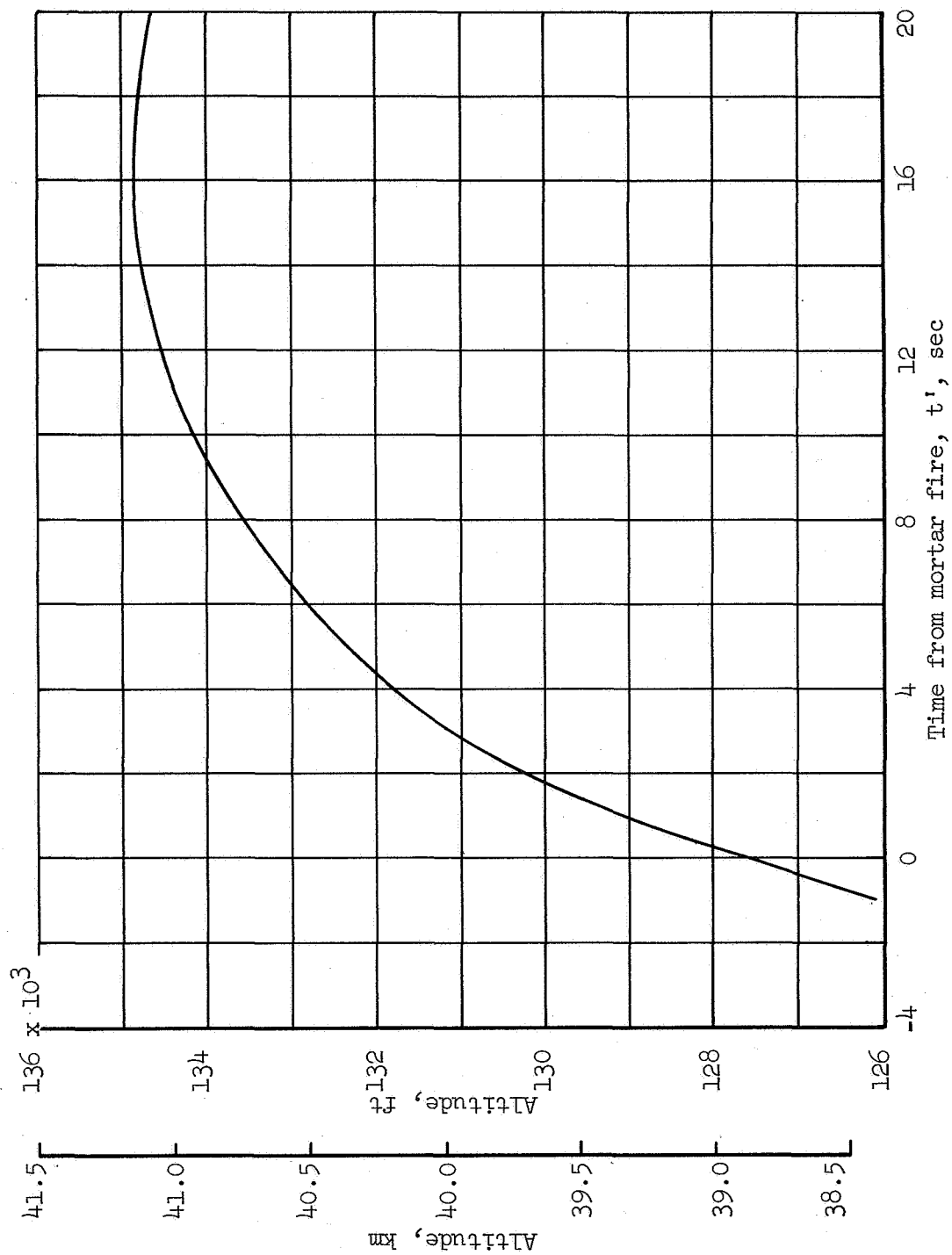


Figure 12.- Altitude time history.

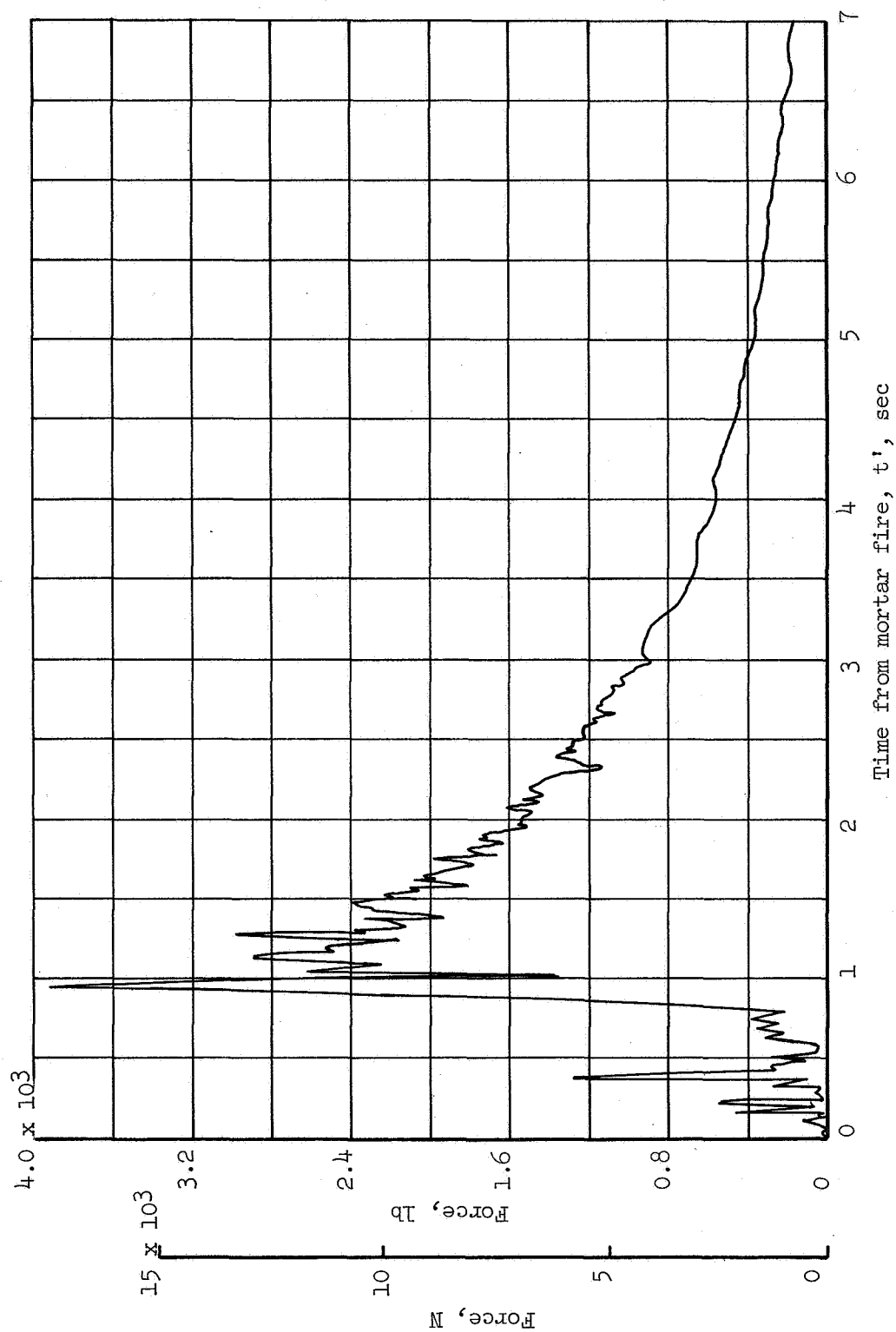


Figure 13.- Tensiometer force time history.

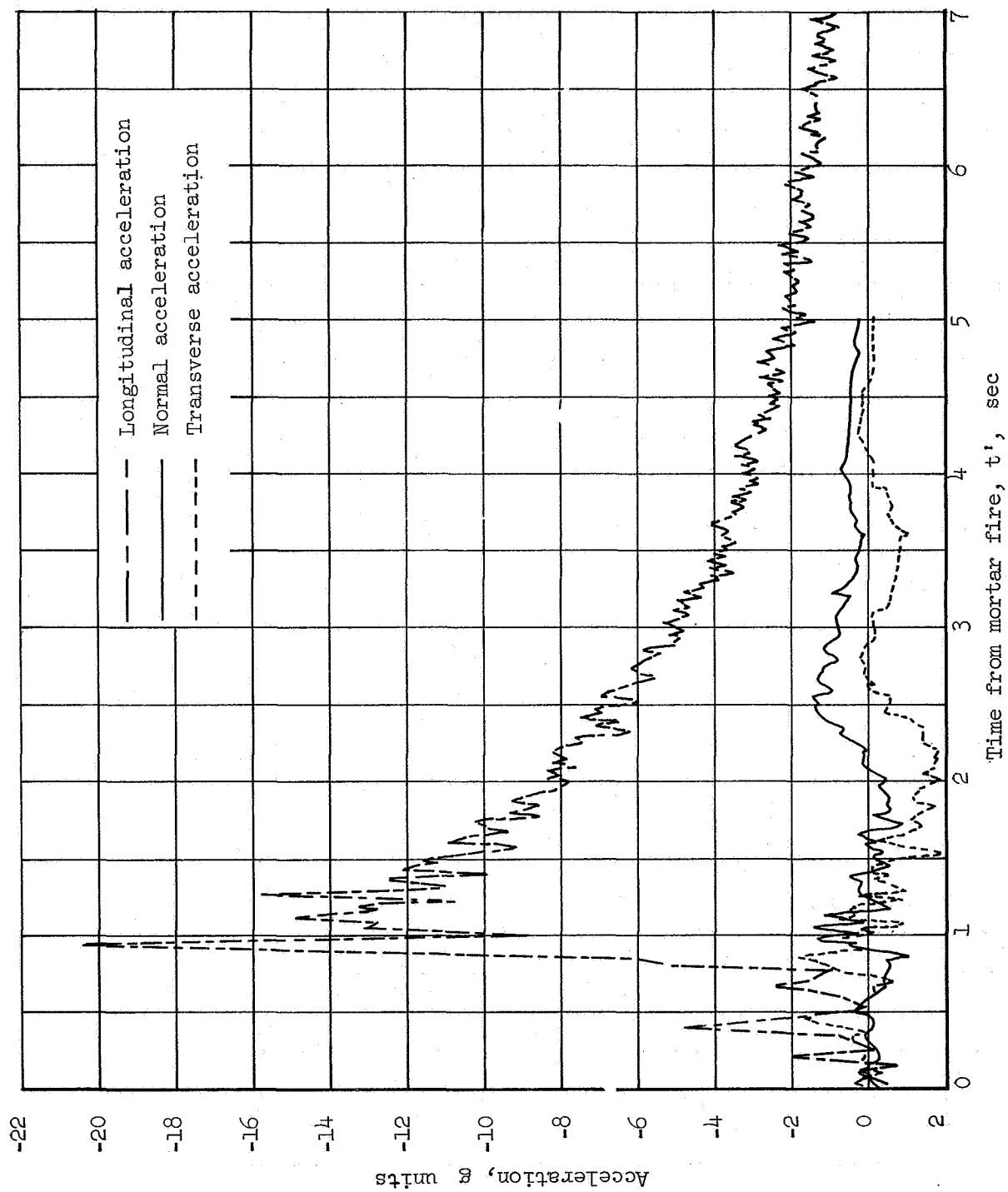
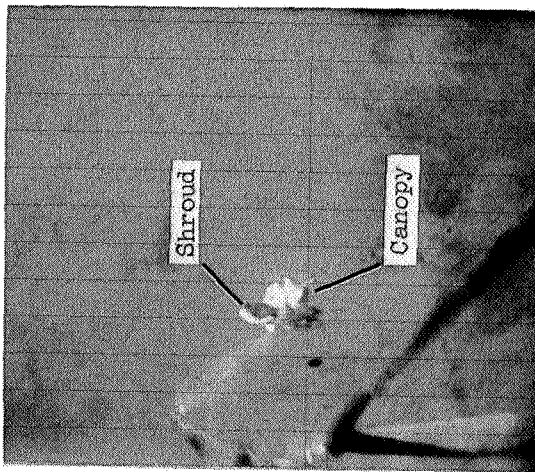
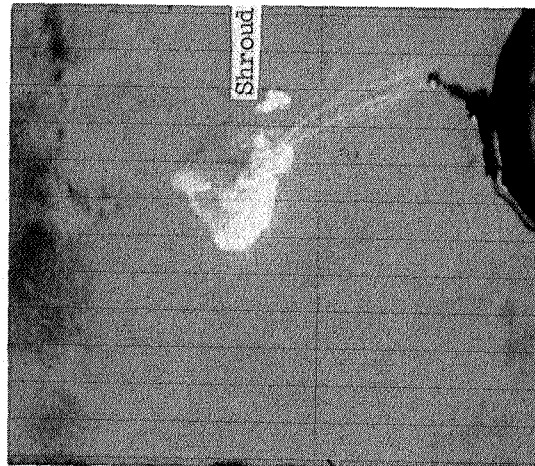


Figure 14.- Acceleration time histories.



$t' = 0.49 \text{ sec}$



$t' = 0.60 \text{ sec}$

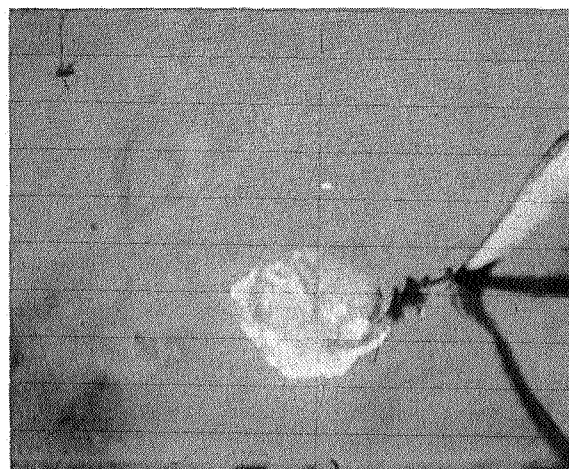


$t' = 0.73 \text{ sec}$

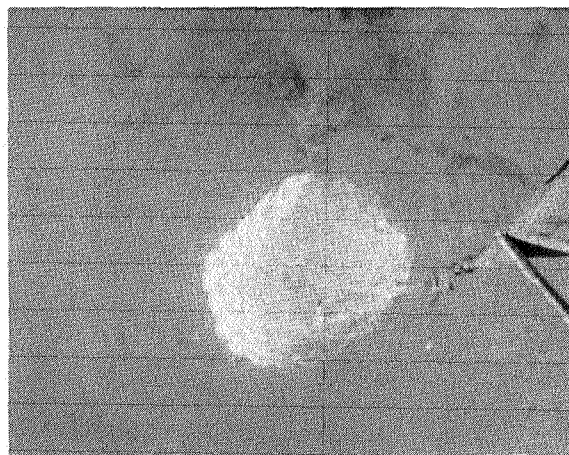
(a) Canopy inflation.

Figure 15.- Onboard camera photographs.

L-67-6625



$t' = 0.80 \text{ sec}$



$t' = 0.87 \text{ sec}$

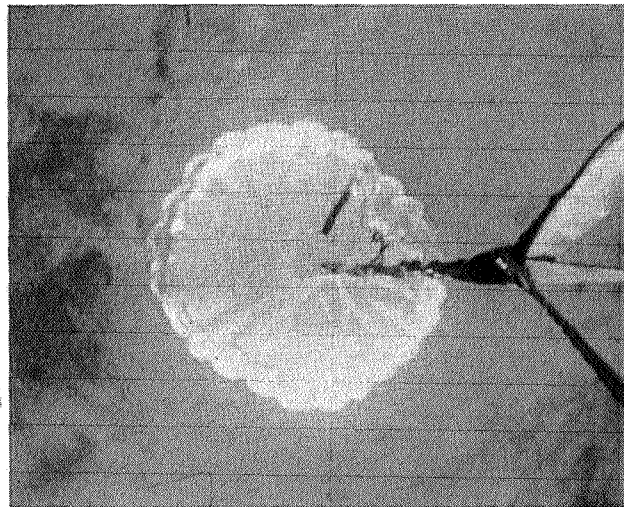


$t' = 0.94 \text{ sec}$

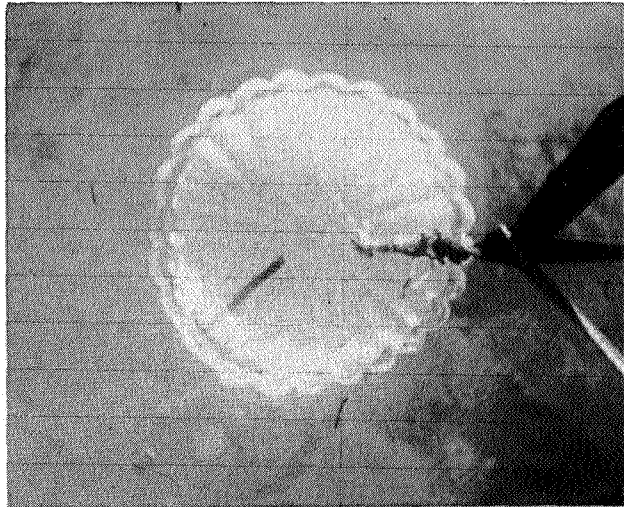
(a) Concluded.

Figure 15.- Continued.

L-67-6626



$t' = 1.02 \text{ sec}$

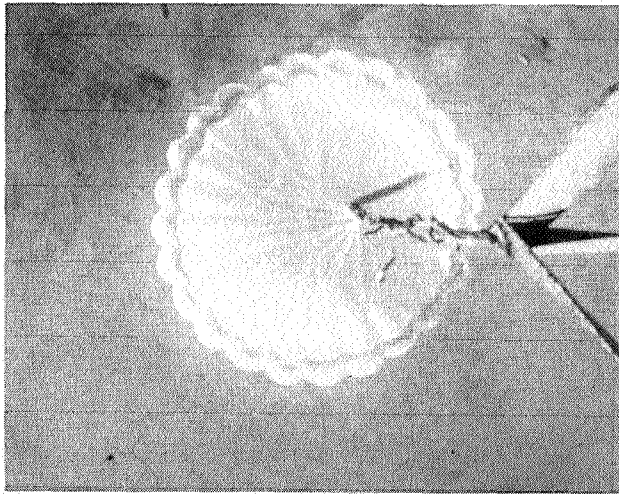


$t' = 1.15 \text{ sec}$

L-67-6627

(b) Canopy shape variations.

Figure 15.- Continued.



$t' = 1.27 \text{ sec}$

(c) Stable inflation. L-67-6628

Figure 15.- Concluded.

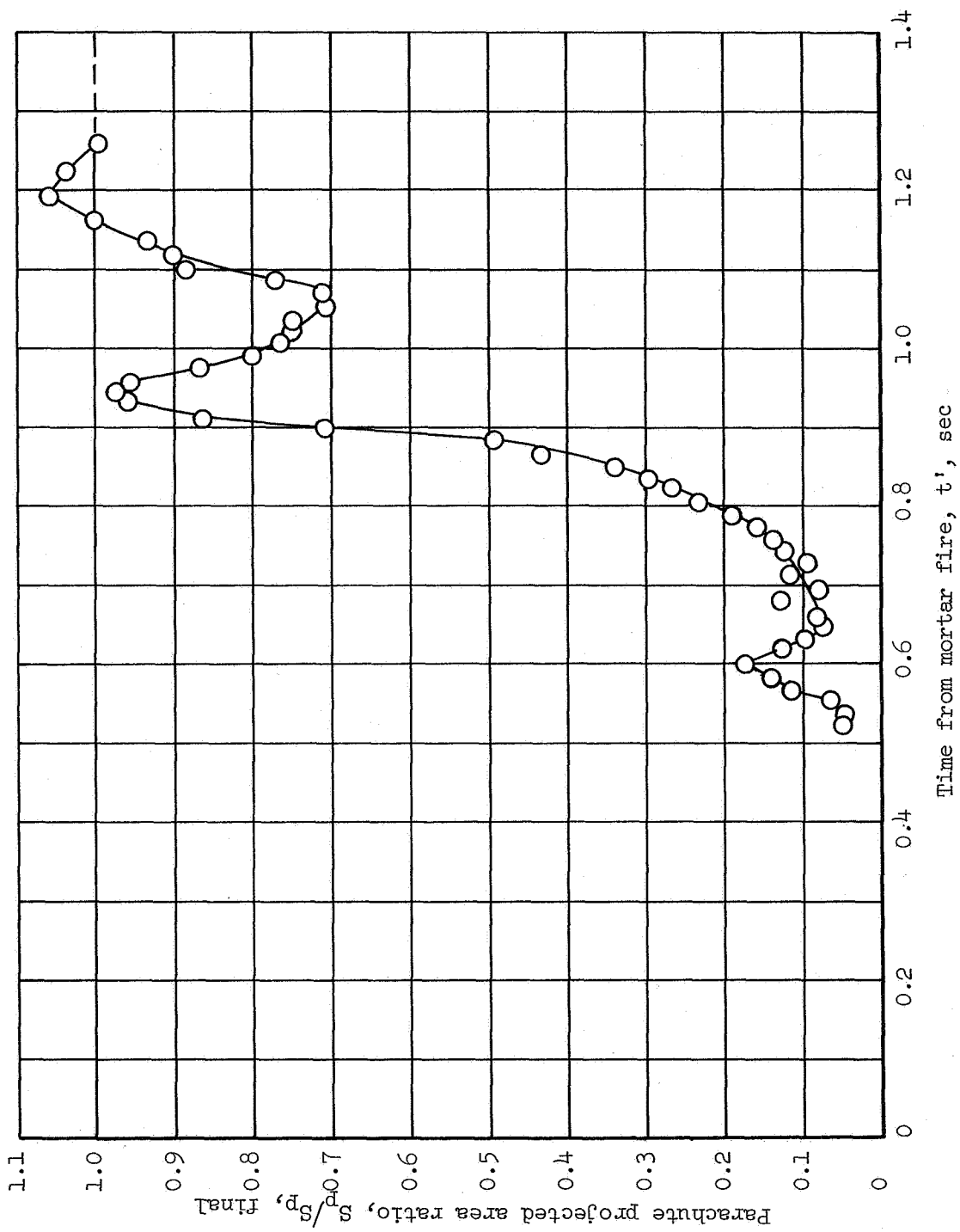


Figure 16.- Parachute projected-area-ratio time history.

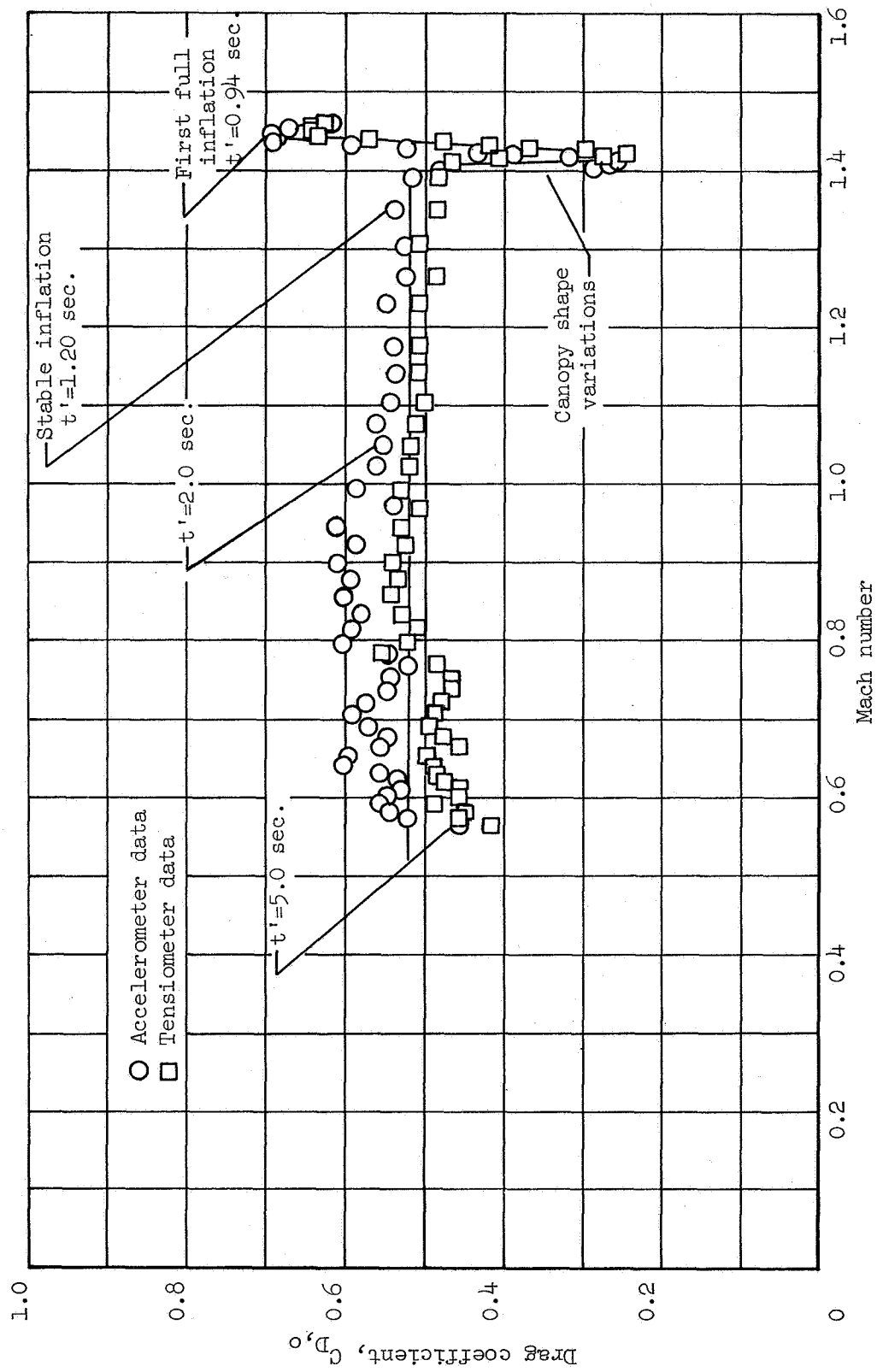


Figure 17.- Variation of parachute drag coefficient with Mach number.

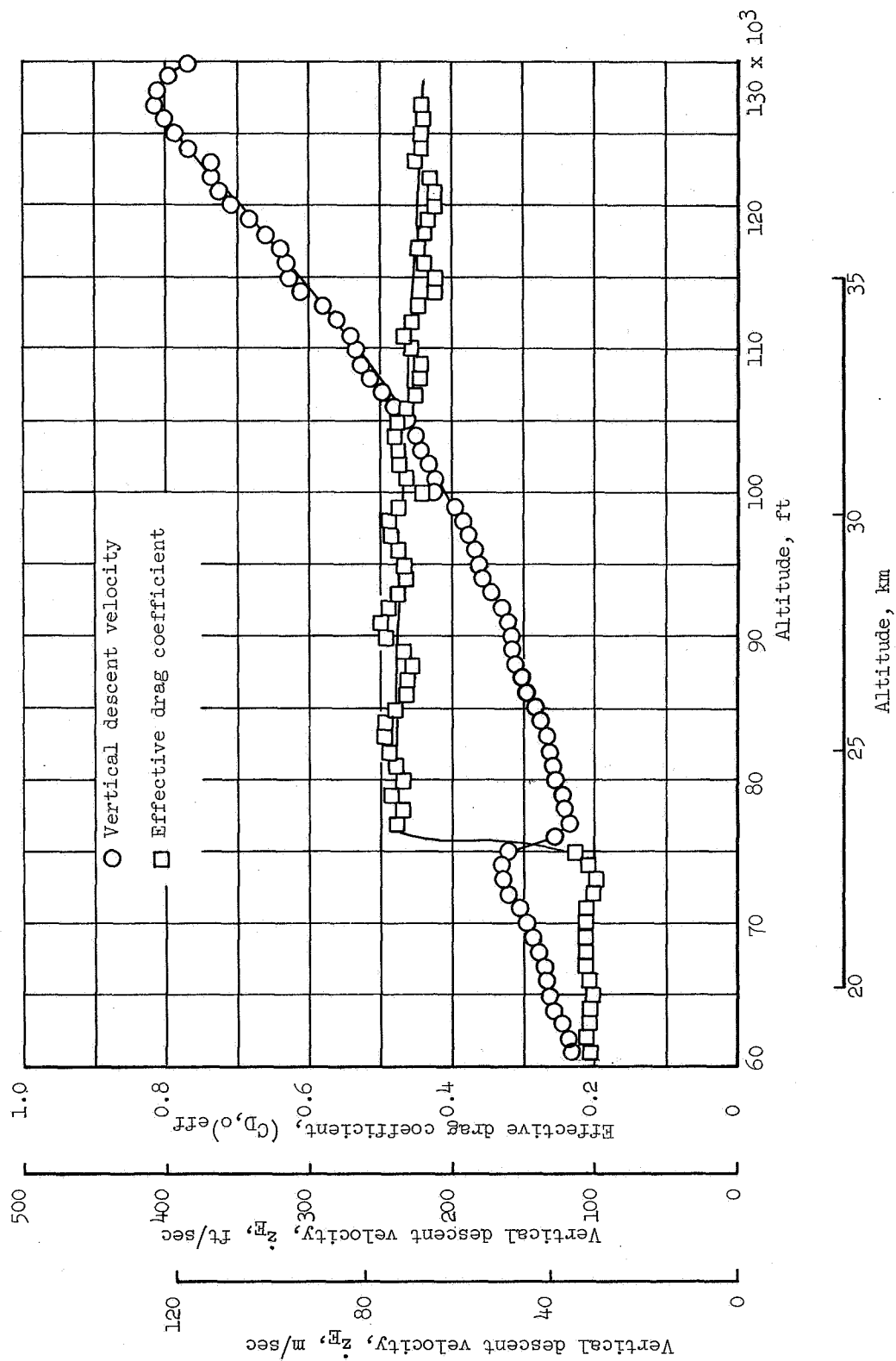


Figure 18.- Variation of vertical descent velocity and effective drag coefficient with altitude.

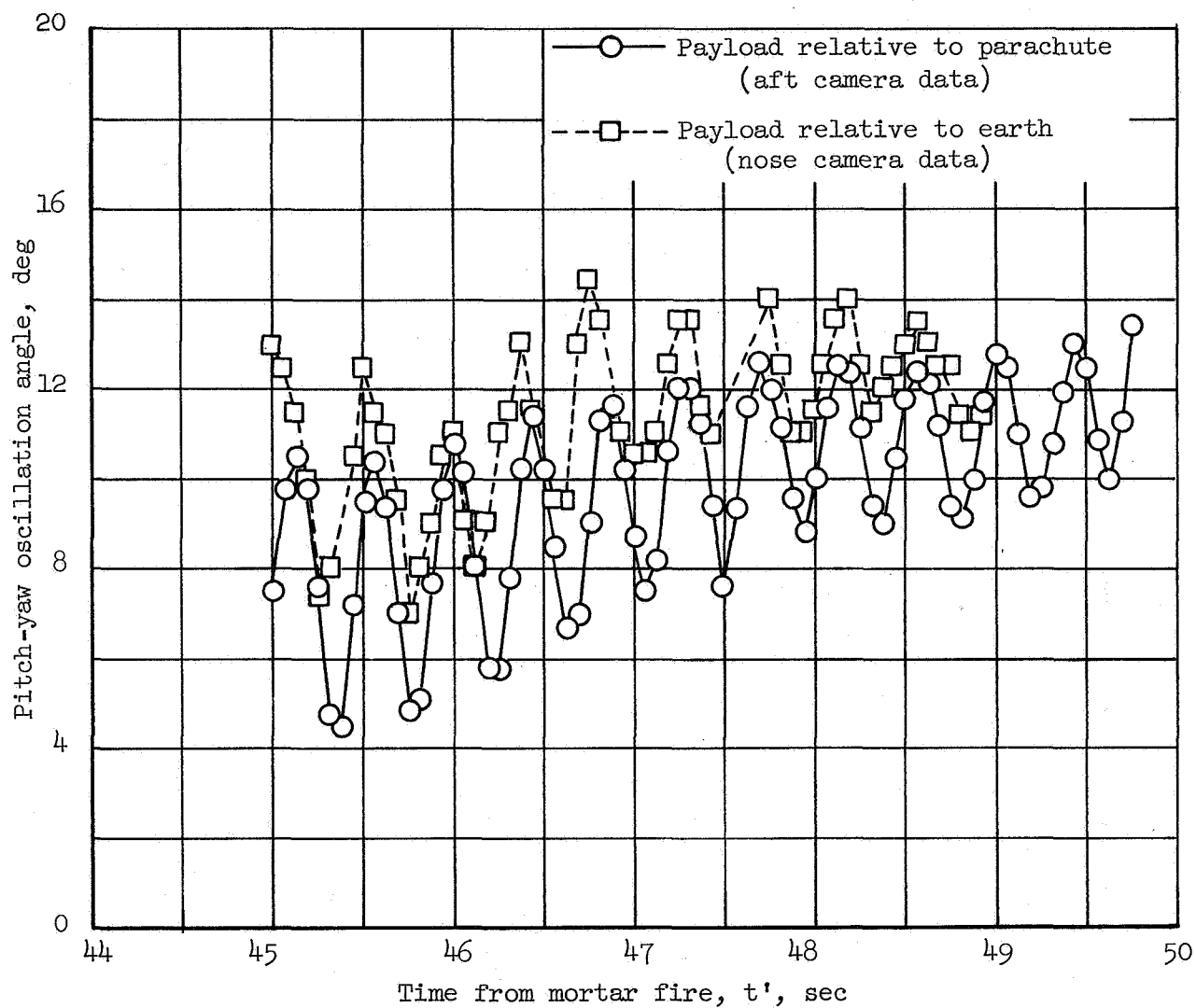


Figure 19.- Time histories of oscillation angles of payload relative to parachute canopy and of payload relative to earth during the initial stages of terminal descent.

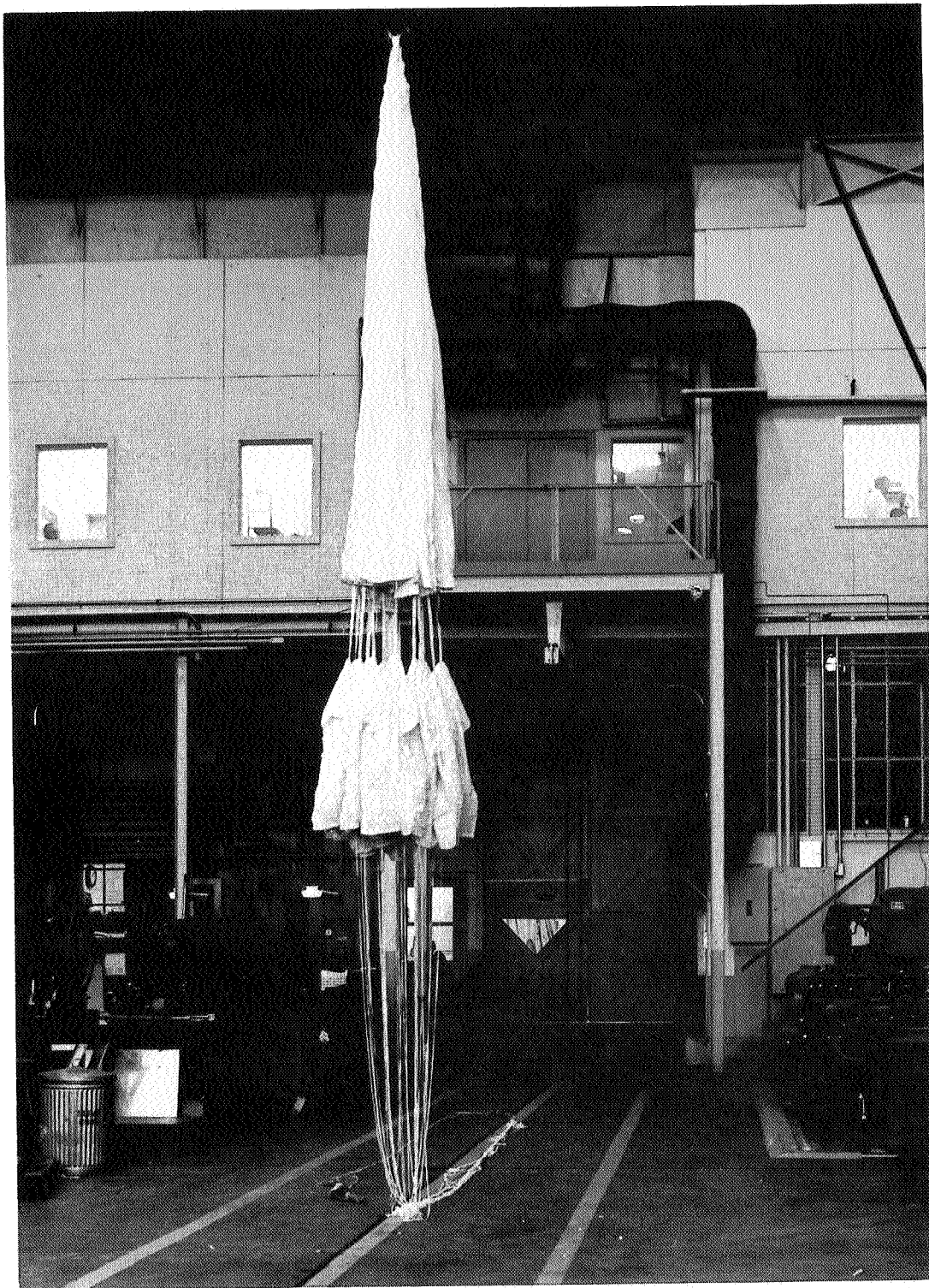


Figure 20.- Photograph of recovered parachute.

L-67-1236

A motion-picture film supplement L-968 is available on loan. Requests will be filled in the order received. You will be notified of the approximate date scheduled.

The film (16 mm, 4 min, color, silent) shows the parachute deployment, inflation, and the deceleration period immediately following deployment. The film, which was obtained from a camera pointed aft from the payload, was taken at a speed of 64 frames per second. The parachute remained supersonic for 2.15 seconds and the apogee altitude of 134 800 feet was attained in 16 seconds after parachute deployment was initiated.

Requests for the film should be addressed to:

Chief, Photographic Division
NASA Langley Research Center
Langley Station
Hampton, Va. 23365

CUT

Date _____

Please send, on loan, copy of film supplement L-968 to
TM X-1451

Name of organization

Street number

City and State

Zip code

Attention: Mr. _____

Title _____

Place
Stamp
Here

Chief, Photographic Division
NASA Langley Research Center
Langley Station
Hampton, Va. 23365